Quaternary Research 85 (2016) 87–93

Contents lists available at ScienceDirect

Quaternary Research

journal homepage: www.elsevier.com/locate/yqres

Variability of ^{14}C reservoir age and air–sea flux of CO_2 in the Peru–Chile upwelling region during the past 12,000 years

Matthieu Carré [a,*], Donald Jackson [b], Antonio Maldonado [c], Brian M. Chase [a], Julian P. Sachs [d]

[a] Institut des Sciences de l'Evolution, Université de Montpellier, CNRS, IRD, EPHE, place Eugène Bataillon, 34095 Montpellier, France
[b] Departamento de Antropología, FACSO, Universidad de Chile, Ignacio Carrera Pinto 1045, Ñuñoa, Santiago, Chile
[c] Centro de Estudios Avanzados en Zonas Aridas (CEAZA), Universidad de La Serena, Casilla 599, La Serena, Chile
[d] School of Oceanography, University of Washington, Box 355351, Seattle, WA 98195, USA

ARTICLE INFO

Article history:
Received 6 May 2015
Available online 9 January 2016

Keywords:
Humboldt system
Reservoir age
Shell middens
Deglaciation
Radiocarbon
CO_2

ABSTRACT

The variability of radiocarbon marine reservoir age through time and space limits the accuracy of chronologies in marine paleo-environmental archives. We report here new radiocarbon reservoir ages (ΔR) from the central coast of Chile (~32°S) for the Holocene period and compare these values to existing reservoir age reconstructions from southern Peru and northern Chile. Late Holocene ΔR values show little variability from central Chile to Peru. Prior to 6000 cal yr BP, however, ΔR values were markedly increased in southern Peru and northern Chile, while similar or slightly lower-than-modern ΔR values were observed in central Chile. This extended dataset suggests that the early Holocene was characterized by a substantial increase in the latitudinal gradient of marine reservoir age between central and northern Chile. This change in the marine reservoir ages indicates that the early Holocene air–sea flux of CO_2 could have been up to five times more intense than in the late Holocene in the Peruvian upwelling, while slightly reduced in central Chile. Our results show that oceanic circulation changes in the Humboldt system during the Holocene have substantially modified the air–sea carbon flux in this region.

Introduction

Extending over 5000 km from the equator to ~50°S, the Peru–Chile coastal upwelling region is the longest eastern boundary upwelling system in the world. The Peru–Chile coastal upwelling plays a significant role in the global carbon cycle, being a highly productive area (Chavez et al., 2008) as well as one of the most intense carbon sources of the global coastal ocean (Laruelle et al., 2010). There is growing evidence that eastern boundary upwelling systems are intensifying with global warming (Bakun, 1990; McGregor et al., 2007; García-Reyes and Largier, 2010; Narayan et al., 2010; Gutiérrez et al., 2011). In addition, climate model simulations recently projected a change in upwelling spatial structure with future intensification being larger at high latitudes than at low latitudes (Wang et al., 2015). Assessing current changes in upwelling systems requires knowledge of their natural temporal and spatial variability.

The Humboldt Current system is complex, involving water masses from the Pacific Equatorial undercurrent in the north and subantarctic surface and intermediate waters in the South, which are characterized by different $\Delta^{14}C$ values (Toggweiler et al., 1991; Strub et al., 1998). The difference in the ^{14}C age of dissolved inorganic carbon (DIC) in marine surface waters relative to the ^{14}C age of contemporaneous terrestrial carbon in equilibrium with the atmosphere is referred to as the marine radiocarbon reservoir age (R) and is due to the residence time of carbon in the ocean. Today, the average marine radiocarbon reservoir age in the ocean mix layer is assumed to be 400 yr by convention. For the past 10,500 years, the Marine13 radiocarbon calibration dataset (Reimer et al., 2013) includes a radiocarbon reservoir age calculated using the atmospheric ^{14}C calibration curve IntCal13 and an ocean–atmosphere box diffusion model (Reimer et al., 2013). Although the model is simplified, the calculated marine radiocarbon curve is consistent with independent estimates from marine archives (Reimer et al., 2013). From 10.5 to 13.9 cal ka BP, the marine radiocarbon calibration includes data from Cariaco Basin varved sediments and from corals (Reimer et al., 2013). Local deviations from the global reservoir age (ΔR), however, vary in space and time with oceanic circulation.

Surface waters off Peru and northern Chile are typically characterized by large marine reservoir ages owing to the upwelling of ^{14}C-depleted deep waters. ΔR values may change on seasonal (Jones et al., 2007, 2010) to multi-millennial time scales as a function of variations in upwelling intensity and/or the origin of the upwelled waters (Toggweiler et al., 1991; Fontugne et al., 2004; Ortlieb et al., 2011). Modern and past ΔR estimates are scarce in the southeast Pacific. On the Chilean coast south of 24°S, only two estimates of pre-bomb ΔR are available today in the 14CHRONO marine reservoir database (http:// http://calib.qub.ac.uk/marine/). A few estimates of Holocene ΔR are available from sediment cores collected off southern Chile

* Corresponding author.
E-mail address: matthieu.carre@umontpellier.fr (M. Carré).

http://dx.doi.org/10.1016/j.yqres.2015.12.002
0033-5894/

(De Pol-Holz et al., 2010, Van Beek et al., 2002; Siani et al., 2013) and none from the coast. Therefore, the uncertainty in ΔR is considerable along ~3600 km of coast, which is a significant limitation on the accurate ^{14}C-dating of ancient sedimentological, biological, or archeological materials of marine origin.

Here we provide new estimates of ΔR over the past 12,000 years in central Chile (31°S–33°S) from paired charcoal and mollusk shells collected in archeological shell middens in the area of Los Vilos. The coast in this area is open to the ocean and does not show any local oceanographic feature or any large river system, so we can consider it as representative of the coastal Humboldt system at this latitude. A comparison with reconstructions from southern Peru and northern Chile compiled by Ortlieb et al. (2011) provides new insights into the spatial structure variability of the globally significant Peru–Chile coastal upwelling system. Based on an empirical relationship between ^{14}C reservoir age and pCO_2 in the southeast Pacific, we discuss the implications for past variability of air–sea CO_2 exchange in this region.

Material and methods

A pre-bomb radiocarbon reservoir age value was estimated from a *Mesodesma donacium* shell collected in Valparaiso and deposited in Paris at the National Museum of Natural History in 1837. This modern reservoir age value might be slightly overestimated since this shell had probably been collected a few years earlier. Holocene ΔR values were estimated from ^{14}C dates of paired mollusk shells and charcoal fragments collected in seven archeological shell middens close to Los Vilos (31.9°S, 71.5°W), on the central coast of Chile (Fig. 1, Table 1). Details on hunter-gatherer archeological occupations around Los Vilos can be found in Jackson (2002) and Méndez and Jackson (2004, 2006). Some authors recommend dating multiple pairs so that contemporaneity of samples can be statistically tested (Russell et al., 2011), which was not possible here. However, the risk of non-contemporaneity was here minimized by a careful control of the archeological context and the stratigraphy. Shell middens used in this study, except for one site (Ñague, Table 1), were thin lenses resulting from ephemeral occupations lasting approximately one season. We selected these sites to ensure a contemporaneous deposition of charcoal and shells. In the Ñague middens, contemporaneity was ensured by selecting shells that were collected in the stratigraphy between two charcoal fragments that yielded statistically undistinguishable radiocarbon dates (Table 1).

The estimate of a marine reservoir age can be biased if the charcoal fragment comes from a tree that died centuries before being used as fuel. This issue, referred to as the "old wood" effect, can be relatively common in the hyper arid coast of Peru (Kennett et al., 2002). While charcoal fragments are sometimes older than associated shells in northern Chile due to the old wood effect and must thus be discarded (Ortlieb et al., 2011), this was not observed in any pair analyzed in central Chile. This risk is mitigated in the central coast as compared to the Atacama desert because central Chile is much less arid, and so dead trees are not as well preserved as in the Atacama desert. Plant species could not be determined from charcoal fragments. However, we minimized the risk of old wood bias by analyzing two charcoal fragments when possible.

We used shell fragments from the same species, *M. donacium*, to minimize variability related to microhabitat or to biological effects. *M. donacium* is a filter-feeder bivalve living in the intertidal to subtidal zone of high energy sand beaches of Peru and Chile (Tarifeño, 1980). Filter feeders are considered to be in equilibrium with dissolved inorganic carbon and thus well suited for ΔR reconstructions (Petchey and Ulm, 2012). Seasonal changes in coastal upwelling can result in substantial

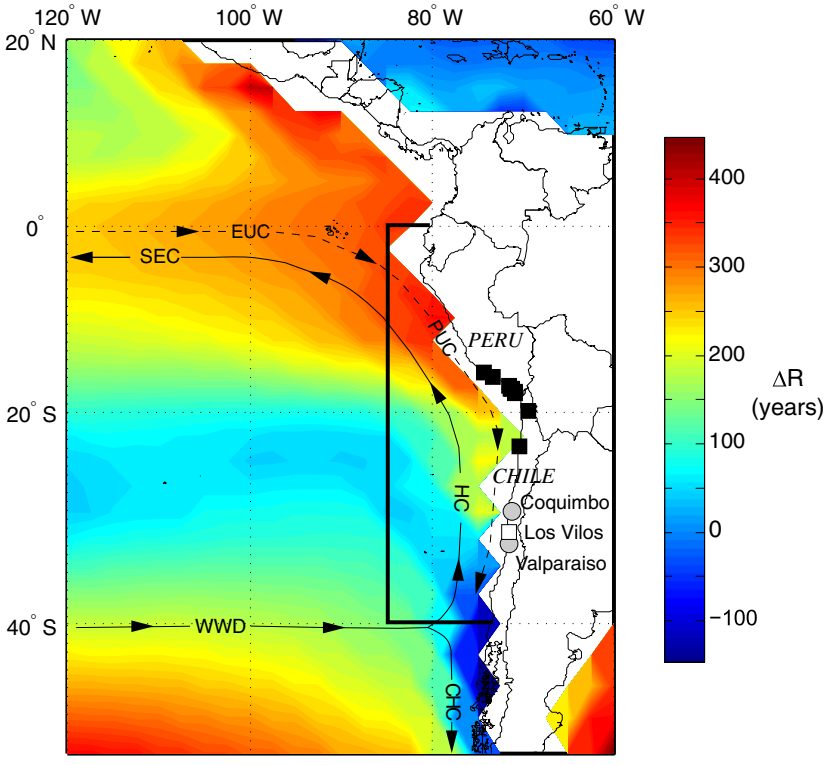

Figure 1. Map of the study region showing simulated marine reservoir age deviations (ΔR, years) of surface water (Butzin et al., 2012) in modern pre-bomb conditions. A simplified representation of ocean circulation (continuous arrows for surface currents and dashed arrows for undercurrents) based on Strub et al. (1998) indicates the South Equatorial current (SEC), the Equatorial undercurrent (EUC), the Peruvian undercurrent (PUC) (which feeds coastal upwelling), the Humboldt current (HC) (also called the Peruvian current), the West Wind drift (WWD), and the Cape Horn current (CHC). We show the sites for modern pre-bomb reservoir age estimates (gray circles), published Holocene reservoir age estimates in southern Peru and northern Chile (black squares) (Southon et al., 1995; Kennett et al., 2002; Owen, 2002; Fontugne et al., 2004; Ortlieb et al., 2011), and Los Vilos, the site for Holocene reservoir age estimates in central Chile (this study, open square). The thick black line shows the area considered for the calculation of the relationship between pCO_2 and ΔR (Fig. 3).

https://doi.org/10.1016/j.yqres.2015.12.002 Published online by Cambridge University Press

Table 1
Radiocarbon dates, reservoir ages, and $\Delta^{14}C$ of surface water in central Chile.

Sample	Material	Lab Ref.	$\delta^{13}C$ (‰ V-PDB)	^{14}C age (yr BP)	Mean ^{14}C age (yr BP)	1σ range (Cal yr BP)	ΔR (yr)	$\Delta^{14}C$ (‰)
Modern pre-bomb samples								
Coquimbo (29.9°S) collection: AD 1837	Marine shell	UCIAMS-142533	[a]	605 ± 25		113–133	146 ± 25	−58.6 ± 4.1
Valparaiso (33.1°S) collection: AD 1939 (Ingram and Southon, 1996)	Marine shell	CAMS-17919/1	2.0	520 ± 50		11	43 ± 52	−61.4 ± 5.8
Valparaiso (33.1°S) collection: AD 1935 (Taylor and Berger, 1967)	Marine shell	UCLA-1278	1.3	770 ± 76		15	303 ± 77	−89.8 ± 8.6
Holocene samples from Los Vilos (31.9°S)								
LV007-N2	Marine shell	OS-63180	1.3	3560 ± 35				
LV007 U3 Capa2	Charcoal	OS-60569	−25.3	3090 ± 40		3182–3339	168 ± 69	−48.4 ± 13.2
Huentelauquen2-N1	Marine shell	Beta-281204	−0.7	6350 ± 40				
Huentelauquen2-N1	Charcoal	Beta-292185	−25.4	6000 ± 40		6732–6857	18 ± 57	31.1 ± 12.9
LV 531 U1 m	Marine shell	CAMS-144653	(0)[b]	8125 ± 30				
LV531 U1 ch	Charcoal	CAMS-144812	(−25)	7780 ± 35*	7830 ± 50	8479–8627	9 ± 45	25.3 ± 13.0
LV531 U1 ch-rep	Charcoal	CAMS-144818	(−25)	7880 ± 25*				
NagueB-N8	Marine shell	OS-63176	0.5	9100 ± 40				
NagueB-N7	Charcoal	OS-60542	−24.2	8690 ± 50	8655 ± 59	9527–9631	169 ± 54	27.2 ± 12.8
NagueB-N10	Charcoal	OS-61907	−24.2	8620 ± 110				
NagueB-N14	Marine shell	OS-63177	1.0	9310 ± 50				
NagueB-N13	Charcoal	OS-61906	−23.3	9190 ± 45*	9190 ± 69	10233–10397	−166 ± 73	94.9 ± 17.6
NagueB-N17	Charcoal	OS-61450	−24.9	9190 ± 130*				
LV079-U2-N1	Marine shell	Beta-293612	−0.9	10,360 ± 50*	10,500 ± 140			
LV079-U2-N9	Marine shell	Beta-293613	0.7	10,640 ± 60*				
LV079-U2-N6	Charcoal	Beta-342528	−24.6	9790 ± 40		11,165–11,228	295 ± 143	47.6 ± 22.3
LV080-U1-N8	Marine shell	Beta-158699	0.4	10,180 ± 70				
LV080-U1-N9	Terr. shell	UGAMS-8849	−10.9	9890 ± 30		11,218–11,263	−95 ± 72	97.3 ± 12.5
PPLV80-N7	Marine shell	OS-63181	0.7	10,400 ± 50				
PPLV80-N6	Charcoal	OS-60566	−24.4	10,050 ± 50*	10,050 ± 37	11,355–11,608	−12 ± 61	99.4 ± 24.7
PPLV80-N9	Charcoal	OS-60559	−24.7	10,050 ± 55*				

* Pooled ages
[a] Value measured on graphite, not shown by lab.
[b] $\delta^{13}C$ values in parenthesis were assumed, not measured.

variations of ^{14}C activity within shells (Jones et al., 2007, 2010). This variability was here averaged out by dating fragments of the shell hinge that integrate most of the mollusk life span (one to four years). The shell hinge is the thickest and best-preserved part of the shell so that original isotopic value is well preserved. Shell recrystalization in *M. donacium* can be diagnosed by direct microscope observation (Carré, 2005; Carré et al., 2014). The dense white and opaque structure and the apparent growth lines observed in the cross-section support the absence of recrystallization in our samples. Shell hinge fragments were mechanically and chemically cleaned to eliminate potentially contaminated surface material. Shell and charcoal fragments were sent to accelerator mass spectrometry (AMS) facilities for radiocarbon dating (Table 1).

^{14}C reservoir age deviations ΔR were calculated from the conventional radiocarbon dates of paired shell and charcoal samples according to the procedure described in Southon et al. (1995), using the SH13 (Hogg et al., 2013) and Marine13 (Reimer et al., 2013) ^{14}C calibration datasets. When two charcoal or two shell ^{14}C dates were available, dates were pooled and the average conventional ^{14}C dates were used for ΔR calculation (Table 1). Pooled dates were statistically identical at 95% confidence level based on Ward and Wilson (1978) chi-square test, except for two cases. First, at the LV079 site, two shells were dated and yielded statistically different ages (Table 1). The archeological context based on excavation observation clearly shows an ephemeral occupation so that shells are likely contemporaneous. Their age difference is thus thought to be a result of seasonal to interannual variability of the coastal upwelling, which justifies their pooling to estimate an average reservoir age. Second, two charcoal dates are statistically different at the LV531-U1 site (Table 1), but these dates are replicates from the same charcoal sample. Since the difference is in this case necessarily due to uncertainties in the analytic procedure, these dates were also pooled. Uncertainty of pooled dates was estimated by the larger of the propagated error or half the difference between the two ages. Propagated uncertainty of ΔR was calculated as described in Russell et al. (2011). Decay-corrected $\Delta^{14}C$ values of marine dissolved inorganic carbon (DIC) were calculated following Stuiver and Polach (1977) and using the 5730 yr ^{14}C half-life.

Deep water masses usually have higher pCO_2 because of the cumulated effect of organic matter mineralization, and lower $\Delta^{14}C$ values (i.e., higher ΔR values) because of limited exchange with atmospheric CO_2. We propose to use this indirect link between ΔR and pCO_2 in our study region to evaluate past changes in surface water pCO_2 associated with changes in ΔR. We thus estimated the modern pre-bomb relationship between pCO_2 and ΔR in the southeast Pacific from the coast to 85°W and from 0 to 40°S (Fig. 1). ΔR was obtained from pre-bomb $\Delta^{14}C$ estimated from total alkalinity by Key et al. (2004). Ocean pCO_2 was calculated from alkalinity and total CO_2 from the Global Data Analysis Project (GLODAP) 1° gridded dataset using equilibrium constants K0 as defined by Weiss (1974), and K1 and K2 as defined by Lueker et al. (2000). Those constants were calculated using a constant salinity value of 35 and water temperature from the World Ocean Atlas (WOA09). Linearly interpolated relationships between pCO_2 and ΔR

https://doi.org/10.1016/j.yqres.2015.12.002 Published online by Cambridge University Press

were obtained in every grid cell along the depth profiles (0 to 100 m, and 0–600 m), and then averaged to obtain a regional model. We used the depth profiles of pCO_2 and ΔR instead of the surface relationship because water chemistry changes in coastal upwelling areas are expected to occur primarily because of changes in the vertical advection (upwelling intensity) rather than horizontal advection.

The pCO_2–ΔR relationship was calculated first using local temperature (at the depth where alkalinity and total CO_2 were measured), and second using sea–surface temperature to account for the change in carbonate chemistry with temperature when deep waters are upwelled to the surface. We use this latter model for a first-order estimate of past pCO_2 changes in our study area, assuming that the pCO_2–ΔR relationship remained similar throughout the Holocene, which will be discussed later. The pCO_2–ΔR relationship was calculated over a region that was limited, so it is relevant to this oceanographic context while being large enough to account for regional variability and get robust statistics.

Results

A pre-bomb (AD 1837) ΔR value of 146 ± 25 yr was obtained at Coquimbo, which lies between previous estimates of 303 ± 77 yr (Taylor and Berger, 1967) and 43 ± 52 yr (Ingram and Southon, 1996), both from Valparaiso. The average modern pre-bomb ΔR value for central Chile is thus 164 ± 131 yr. At 3.2 cal ka BP, a ΔR value of 168 ± 69 yr was obtained in Los Vilos, very close to the modern pre-bomb value (Fig. 2A). The average value obtained for the whole pre-bomb late Holocene is 165 ± 50 yr. In the early to middle Holocene (from 12 to 6 cal ka BP), ΔR values at Los Vilos ranged from −166 ± 73 to 295 ± 143 yr with an average value of 31 ± 156 yr, but they were particularly variable from 11.5 to 9.5 cal ka BP (Fig. 2A). The average ΔR value for the early to middle Holocene is slightly lower compared to the late Holocene, although the difference is not statistically significant at the 95% confidence level.

Surface DIC $\Delta^{14}C$ values calculated in Los Vilos dropped by ~150‰ during the Holocene: from ~85‰ before 10 cal ka BP to ~−65‰ in the late Holocene (Fig. 2B). The reconstructed $\Delta^{14}C$ values closely follow the global trend of decreasing atmospheric radiocarbon activity that began during the deglaciation and continued through the Holocene (Reimer et al., 2013).

We compare here the new ΔR values from central Chile with Holocene ΔR values estimated and compiled by Ortlieb et al. (2011) for southern Peru and northern Chile (from 15°50′S to 23°34′S). Here, ΔR values were recalculated for consistency using SH13 and Marine13 calibration curves, as in Hua et al., (2015). The average ΔR value for the late Holocene, including modern pre-bomb values, is 225 ± 117 yr (Fig. 2), which is slightly higher than the late Holocene value in central Chile. Although this difference is not statistically significant, it is in agreement with simulations (Butzin et al., 2012) (Fig. 1) and with GLODAP estimates based on water alkalinity (Key et al., 2004). On the other hand, the mean ΔR value in the early Holocene is 528 ± 301 yr for southern Peru and northern Chile, which is much higher (statistically significant at 95% confidence level) than the mean ΔR value of 31 ± 156 yr that we obtained in central Chile at 32°S for the same period (Fig. 2).

The modern pre-bomb relationship between pCO_2 and ΔR in the southeast Pacific shows an increasing trend of pCO_2 with ΔR (Fig. 3), that is essentially due to pCO_2 and ΔR increasing in parallel with depth. Based on the model calculated with SST on a 600-m water column, we estimated the surface water pCO_2 in central Chile and southern Peru in modern pre-bomb conditions and in the early Holocene using estimated average ΔR values for these regions and periods. Reconstructed values of past pCO_2 were then compared to pre-industrial atmospheric pCO_2, which remained between 250 and 290 ppm during the Holocene based on ice-core measurements (Monnin et al., 2004). In central Chile, a late Holocene pre-bomb pCO_2 value of 305 ± 59 ppm was estimated, very close to atmospheric CO_2 concentration. A pCO_2 value could not be estimated for this region for the early Holocene because the ΔR value of 31 yr is beyond the range of this model. In Southern Peru and northern Chile, we obtain a late Holocene pCO_2 value of 516 ± 125 ppm and an early Holocene pCO_2 value of 1576 ± 208 ppm. The error bar here only includes the uncertainty related to the pCO_2–ΔR relationship.

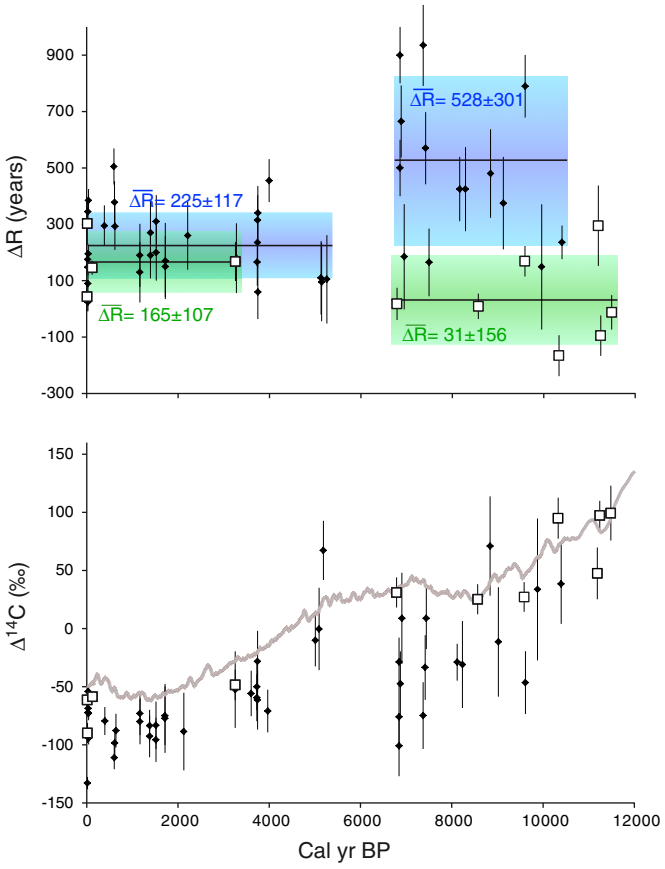

Figure 2. Holocene changes of surface water radiocarbon content in central Chile (green) and in southern Peru/northern Chile (blue). (A) Reservoir age deviation (ΔR) calculated from 12,000 cal yr BP to the modern pre-bomb period in central Chile (32°S) (open squares) compared to values from northern Chile–southern Peru (14–24°S) (black diamonds) compiled by Ortlieb et al. (2011). For consistency with the new data, ΔR values were here recalculated using Marine13 and SH13 calibration curves as in Hua et al. (2015). Mean values and ±1σ intervals are shown for the early Holocene and for the late Holocene in central Chile (green box) and northern Chile–southern Peru (blue box). (B) DIC decay-corrected $\Delta^{14}C$ calculated values from central Chile and northern Chile–southern Peru. The Marine13 calibration curve (Reimer et al., 2013) is shown in gray.

Discussion

These ΔR values from Los Vilos archeological sites are the first estimates of Holocene radiocarbon reservoir age in central Chile. They will help in improving radiocarbon-based chronologies of coastal archeological sites and paleoenvironmental marine archives in this region. Early Holocene ΔR values from central Chile imply a similar or weaker influence of ^{14}C-impoverished deep water, caused by either decreased upwelling or the upwelling of better ventilated water. Sea–surface temperature (SST) reconstructions from the region indicate that temperatures were warmer than today offshore (Kim et al., 2002) and similar along the coast (Carré et al., 2012), suggesting that coastal upwelling in central Chile occurred in a narrower band close to the coast in the early Holocene.

https://doi.org/10.1016/j.yqres.2015.12.002 Published online by Cambridge University Press

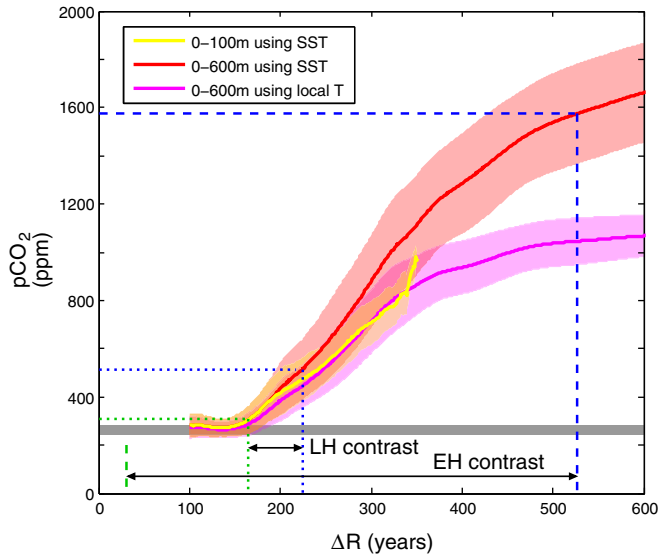

Figure 3. Average relationship between pCO_2 and ΔR (with $\pm 1\sigma$ interval) in the southeast Pacific (area indicated by the thick line in Fig. 1) calculated from GLODAP data (Key et al., 2004) from 0 to 100 m depth using annual SST values (yellow), from 0 to 600 m depth using SST values (red), and from 0 to 600 m depth using local temperature (pink). The Holocene range of atmospheric pCO_2 in Dome C ice core (Monnin et al., 2004) is indicated for comparison by a dark gray band. Late Holocene (dotted lines) and early Holocene (continuous lines) pCO_2 and ΔR are indicated for central Chile (green) and southern Peru (blue). Arrows show the latitudinal contrast in the late Holocene (LH) and early Holocene (EH).

Our new ΔR estimates from central Chile contrast with those obtained in southern Peru and northern Chile, showing high ΔR values of 528 ± 301 yr in the early Holocene (Fontugne et al., 2004; Ortlieb et al., 2011) (Fig. 2A). These high reservoir age values in southern Peru were attributed to vigorous coastal upwelling, an interpretation supported by low $\delta^{13}C$ values in mollusk shells (Sadler et al., 2012) and lower SSTs (Carré et al., 2005, 2014).

The latitudinal contrast in ΔR was much stronger in the early Holocene, which implies a change in the character of the Humboldt system. Today, the waters upwelled off Peru and Chile are transported from the north by the Peru–Chile Undercurrent, which is fed by Equatorial Subsurface Water (ESSW) that has its origins in the lower part of the Equatorial Undercurrent fed by subantarctic mode waters (SAMW) (Toggweiler et al., 1991). These waters are characterized by low $\Delta^{14}C$, low oxygen content and high pCO_2. Fontugne et al. (2004) suggested that the early Holocene increase in coastal ΔR in Peru was too large to result from upwelling enhancement alone and required that upwelled waters were more ^{14}C-depleted. Lower $\Delta^{14}C$ values of upwelled waters could have resulted from a longer residence time, or from a larger contribution of SAMW in the Equatorial undercurrent. This hypothesis was discussed by Hua et al. (2015), who observed that the ^{14}C marine reservoir age increased during the early Holocene in the Western and in the eastern tropical Pacific. It is supported by a comparison between ocean model simulations and a coral $\Delta^{14}C$ record in the Galapagos, which showed that $\Delta^{14}C$ modern variability in the eastern tropical Pacific is primarily controlled by changes in the SAMW component in the upwelling water (Rodgers et al., 2004).

Another hypothesis is that the geographic origin of upwelled waters changed, potentially to Antarctic intermediate waters (AAIW) that are even more ^{14}C-depleted than SAMW. This effect was not observed in central Chile. The influence of the Peru–Chile undercurrent decreases southward as its water mixes with the Humboldt Current that transports oxygen-rich Subantarctic Surface Water (SSW) northward (Silva et al., 2009). Today, this front is observed at 36.5°S and is characterized by an abrupt transition of the air–sea CO_2 flux (Torres et al., 2011). In the early Holocene, the slightly lower ΔR values at 32°S and the stronger latitudinal gradient between northern and central Chile implies that the front between ESSW and SSW was likely located north of its modern position.

In a marine sediment core collected at ~1000 m depth at 46°S, a sea-surface ^{14}C reservoir age increase of ~100 yr was estimated at ca. 11.5 cal ka BP compared to late Holocene conditions (Siani et al., 2013). In a sediment core located farther south at 53°S, within the influence of the Antarctic Circumpolar Current, Van Beek et al. (2002) estimated a ^{14}C reservoir age increase of ~900 yr at ca. 9.5-cal ka BP compared to the middle and late Holocene, which was interpreted as evidence for a stronger influence of AAIW. Similar trends are thus observed in the southern coast of Chile and in southern Peru, while at the same time ΔR along the central coast seemed unaffected. This suggests that changes in southern Peru and southern Chile were not connected through the Humboldt system.

The Humboldt system, from the equator to ~36°S, is the most intense carbon source of the global coastal ocean (Laruelle et al., 2010); whereas south of 36.5°S, Chilean coastal waters become a carbon sink (Torres et al., 2011). Changes in the gradient of ΔR in the Peru–Chile upwelling region therefore imply changes in the latitudinal character of air–sea CO_2 exchange. Air–sea CO_2 flux is proportional to ΔpCO_2, the difference between surface-water pCO_2 and atmospheric pCO_2. Past ΔpCO_2 can be estimated from atmospheric pCO_2 reconstructed from ice cores, and from marine pCO_2 reconstructed here from ΔR values using the pCO_2–ΔR relationship calculated for the southeast Pacific (Fig. 3).

In central Chile, the late Holocene ΔR value (165 ± 107 yr) indicates a seawater ΔpCO_2 of about 30 ppm, which is lower than recent measurements (Torres et al., 2011). However, the late Holocene pCO_2 of 516 ± 125 ppm estimated for southern Peru and northern Chile (Fig. 3) is within the range of pCO_2 values measured in Peru (~400 to 1000 ppm) and close to the average value of about 600 ppm (Friederich et al., 2008). This result supports the accuracy of the model for the Peruvian area and suggests that average ΔR values estimated from shell hinges integrate and average out the high temporal and spatial variability. ΔpCO_2 was thus about 250 ppm in southern Peru in the late Holocene, which means that waters in Peru were a very intense carbon source. Assuming that the model was still valid in the early Holocene, ΔpCO_2 was about 1300 ppm in Peru during that period, which suggests that CO_2 outgassing might have been five times more intense in average. Based on the relationship between pCO_2 and SST observed in Peru (Friederich et al., 2008) and Holocene SST reconstructions in southern Peru (Carré et al., 2014), we can independently estimate that the sea-to-air CO_2 flux in southern Peru during the early Holocene was twice the modern value. Today that flux is 5.1 mol/m^2/yr in Peru (Friederich et al., 2008) and 2.7 mol/m^2/yr in Chile from Iquique (21°S) to Concepcion (36°S) (Paulmier et al., 2008). The CO_2 flux may have reached ~10 to 25 mol/m^2/yr in Peru during the early Holocene, while it was unchanged or slightly lower than today in central Chile.

These estimates only yield indications about the order of magnitude of past air–sea flux changes in the Peru–Chile upwelling system. Their accuracy is limited (1) by the fact that the water $\Delta^{14}C$ and pCO_2 depth profiles were likely different in the early Holocene, and (2) by the large variability of reconstructed ΔR values. It is interesting to note that early Holocene ΔR values in central Chile and in southern Peru are, respectively, below and above the range of values observed today in the region in the 0–100 m water column (Fig. 3). This strongly supports the hypothesis of Fontugne et al. (2004) that upwelling alone cannot account for these changes, and so which must also involve a change in the origin of the upwelled water.

Conclusions

Radiocarbon dates of contemporaneous marine shells and charcoal fragments collected in coastal archeological deposits near Los Vilos, Chile (31.9°S, 71.5°W) provided estimates of marine reservoir ages

https://doi.org/10.1016/j.yqres.2015.12.002 Published online by Cambridge University Press

during the past 12,000 years. A mean ΔR value of 165 ± 107 yr was obtained for the late Holocene conditions, while a value of 31 ± 156 was obtained for the early to middle Holocene (12 to 6 cal ka BP). Farther north on the southern Peru and northern Chile coast, higher ΔR values in the early Holocene imply an increase in upwelling intensity combined with the upwelling of poorly ventilated water (Fontugne et al., 2004; Carré et al., 2005, 2014; Ortlieb et al., 2011; Hua et al., 2015). A similar trend was also observed off the southern coast of Chile (Van Beek et al., 2002; Siani et al., 2013). The early Holocene is thus characterized by a large latitudinal gradient in $\Delta^{14}C$ of DIC, which indicates a substantial difference in the structure of the Humboldt system in the early, as compared to the late, Holocene. While southern Peru and southern Chile seemed to be more influenced in the early Holocene by SAMW and AAIW respectively, these influences may have been disconnected since they did not reach our study area at ~32°S. Based on the modern relationship between ΔR and seawater pCO_2 in the southeast Pacific, we project that the Peruvian upwelling CO_2 emission to the atmosphere was two to five times more intense in the early Holocene as upwelling was intensified and brought a more CO_2-rich (and ^{14}C-depleted) water mass to the surface. At the same period, the air–sea CO_2 flux in central Chile was similar to modern conditions or slightly weaker.

These results, while allowing for better radiocarbon chronologies of marine material in central Chile, show profound changes in the oceanic circulation within the Humboldt system during the Holocene, which were associated with large changes in the air–sea CO_2 flux in this area.

Acknowledgments

This research was supported by the National Geographic Society under grant no. 8122-06 (M.C.), the U.S. National Science Foundation under grant no. NSF-ATM-0811382 (J.P.S.), and the Chilean FONDECYT under grant no. 1140824 (D.J.). We are thankful to Robert M. Key for providing the GLODAP data, to Martin Butzin for providing the simulated radiocarbon data. We thank Rachid Cheddadi, Associate Editor Tom Marchitto, Senior Editor Derek Booth, and two anonymous reviewers for their constructive comments.

References

Bakun, A., 1990. Global warming change and intensification of coastal ocean upwelling. Science 247, 198–201.
Butzin, M., Prange, M., Lohmann, G., 2012. Readjustment of glacial radiocarbon chronologies by self-consistent three-dimensional ocean circulation modeling. Earth and Planetary Science Letters 317–318, 177–184.
Carré, M. (2005). "Etude géochimique et sclérochronologique de coquilles de bivalves marins: paléocéanographie de la côte sud du Pérou à l'Holocène inférieur et implications archéologiques." Unpublished PhD thesis, Université Montpellier 2.
Carré, M., Bentaleb, I., Fontugne, M., Lavallée, D., 2005. Strong El Niño events during the early Holocene: stable isotope evidence from Peruvian sea-shells. The Holocene 15, 42–47.
Carré, M., Azzoug, M., Bentaleb, I., Chase, B.M., Fontugne, M., Jackson, D., Ledru, M.-P., Maldonado, A., Sachs, J.P., Schauer, A.J., 2012. Mid-Holocene mean climate in the south-eastern Pacific and its influence on South America. Quaternary International 253, 55–66.
Carré, M., Sachs, J.P., Purca, S., Schauer, A.J., Braconnot, P., Angeles Falcón, R., Julien, M., Lavallée, D., 2014. Holocene history of ENSO variance and asymmetry in the eastern tropical Pacific. Science 345, 1045–1048.
Chavez, F.P., Bertrand, A., Guevara-Carrasco, R., Soler, P., Csirke, J., 2008. The northern Humboldt Current System: Brief history, present status and a view towards the future. Progress In Oceanography 79, 95–105.
De Pol-Holz, R., Keigwin, L., Southon, J., Hebbeln, D., Mohtadi, M., 2010. No signature of abyssal carbon in intermediate waters off Chile during deglaciation. Nature Geoscience 3, 192–195.
Fontugne, M., Carré, M., Bentaleb, I., Julien, M., Lavallée, D., 2004. Radiocarbon reservoir age variations in the south Peruvian upwelling during the Holocene. Radiocarbon 46, 531–537.
Friederich, G.E., Ledesma, J., Ulloa, O., Chavez, F.P., 2008. Air–sea carbon dioxide fluxes in the coastal southeastern tropical Pacific. Progress in Oceanography 79, 156–166.
García-Reyes, M., Largier, J., 2010. Observations of increased wind-driven coastal upwelling off central California. Journal of Geophysical Research, Oceans 115, C04011.
Gutiérrez, D., Bouloubassi, I., Sifeddine, A., Purca, S., Goubanova, K., Graco, M., Field, D., Méjanelle, L., Velazco, F., Lorre, A., Salvatecci, R., Quispe, D., Vargas, G., Dewitte, B., Ortlieb, L., 2011. Coastal cooling and increased productivity in the main upwelling zone off Peru since the mid-twentieth century. Geophysical Research Letters 38.
Hogg, A.G., Hua, Q., Blackwell, P.G., Niu, M., Buck, C.E., Guilderson, T.P., Heaton, T.J., Palmer, J.G., Reimer, P.J., Reimer, R.W., Turney, C.S.M., Zimmerman, S.R.H., 2013. SHCal13 Southern Hemisphere Calibration, 0–50,000 years cal BP. Radiocarbon 55, 1–15.
Hua, Q., Webb, G.E., Zhao, J.X., Nothdurft, L.D., Lybolt, M., Price, G.J., Opdyke, B.N., 2015. Large variations in the Holocene marine radiocarbon reservoir effect reflect ocean circulation and climatic changes. Earth and Planetary Science Letters 422, 33–44.
Ingram, B.L., Southon, J.R., 1996. Reservoir ages in eastern Pacific coastal and estuarine waters. Radiocarbon 38, 573–582.
Jackson, D., 2002. Cazadores y recolectores del holoceno medio del norte semiárido de Chile. Universidad de Chile (Tesis para optar el grado de Magíster en Arqueología).
Jones, K.B., Hodgins, G.W.L., Dettman, D.L., Andrus, C.F.T., Nelson, A., Etayo-Cadavid, M.F., 2007. Seasonal variations in Peruvian marine reservoir age from pre-bomb *Argopecten purpuratus* shell carbonate. Radiocarbon 49, 877–888.
Jones, K.B., Hodgins, G.W.L., Etayo-Cadavid, M.F., Andrus, C.F.T., Sandweiss, D.H., 2010. Centuries of marine radiocarbon reservoir age variation within archaeological *Mesodesma donacium* shells from southern Peru. Radiocarbon 52, 1207–1214.
Kennett, D.J., Ingram, B.L., Southon, J.R., Wise, K., 2002. Differences in ^{14}C age between stratigraphically associated charcoal and marine shell from the archaic period site of kilometer 4, southern Peru: old wood or old water? Radiocarbon 44, 53–58.
Key, R.M., Kozyr, A., Sabine, C.L., Lee, K., Wanninkhof, R., Bullister, J.L., Feely, R.A., Millero, F.J., Mordy, C., Peng, T.H., 2004. A global ocean carbon climatology: results from Global Data Analysis Project (GLODAP). Global Biogeochemical Cycles 18, GB4031.
Kim, J.-H., Schneider, R.R., Hebbeln, D., Müller, P.J., Wefer, G., 2002. Last deglacial sea–surface temperature evolution in the Southeast Pacific the South American continent. Quaternary Science Reviews 21, 2085–2097.
Laruelle, G.G., Dürr, H.H., Slomp, C.P., Borges, A.V., 2010. Evaluation of sinks and sources of CO2 in the global coastal ocean using a spatially-explicit typology of estuaries and continental shelves. Geophysical Research Letters 37, L15607.
Lueker, T.J., Dickson, A.G., Keeling, C.D., 2000. Ocean pCO2 calculated from dissolved inorganic carbon, alkalinity, and equations for K1 and K2: validation based on laboratory measurements of CO2 in gas and seawater at equilibrium. Marine Chemistry 70, 105–119.
McGregor, H.V., Dima, M., Fischer, H.W., Mulitza, S., 2007. Rapid 20th-Century Increase in Coastal Upwelling off Northwest Africa. pp. 637–639.
Méndez, C.A., Jackson, D.G., 2004. Ocupaciones humanas del Holoceno tardío en Los Vilos (IV Región, Chile): origen y características conductuales de la población local de cazadores recolectores de litoral. Chungará Revista de Antropología Chilena 36, 279–293.
Méndez, C.A., Jackson, D.G., 2006. Causalidad o concurrencia, relaciones entre cambios ambientales y sociales en los cazadores recolectores durante la transición entre el Holoceno medioy tardío (coasta del semiárido de Chile). Chungará Revista de Antropología Chilena 38, 172–184.
Monnin, E., Steig, E.J., Siegenthaler, U., Kawamura, K., Schwander, J., Stauffer, B., Stocker, T.F., Morse, D.L., Barnola, J.-M., Bellier, B., Raynaud, D., Fischer, H., 2004. Evidence for substantial accumulation rate variability in Antarctica during the Holocene, through synchronization of CO2 in the Taylor Dome, Dome C and DML ice cores. Earth and Planetary Science Letters 224, 45–54.
Narayan, N., Paul, A., Mulitza, S., Schulz, M., 2010. Trends in coastal upwelling intensity during the late 20th century. Ocean Science 6, 815–823.
Ortlieb, L., Vargas, G., Saliège, J.-F., 2011. Marine radiocarbon reservoir effect along the northern Chile-southern Peru coast (14–24°S) throughout the Holocene. Quaternary Research 75, 91–103.
Owen, B.D., 2002. Marine carbon reservoir age estimates for the far south coast of Peru. Radiocarbon 44, 701–708.
Paulmier, A., Ruiz-Pino, D., Garcon, V., 2008. The oxygen minimum zone (OMZ) off Chile as intense source of CO2 and N2O. Continental Shelf Research 28, 2746–2756.
Petchey, F., Ulm, S., 2012. Marine reservoir variation in the Bismarck region: an evaluation of spatial and temporal change in ΔR and R over the last 3000 years. 54 pp. 45–58.
Reimer, P.J., Bard, E., Bayliss, A., Beck, J.W., Blackwell, P.G., Bronk Ramsey, C., Buck, C.E., Cheng, H., Edwards, R.L., Friedrich, M., Grootes, P.M., Guilderson, T.P., Haflidason, H., Hajdas, I., Hatté, C., Heaton, T.J., Hoffmann, D.L., Hogg, A.G., Hughen, K.A., Kaiser, K.F., Kromer, B., Manning, S.W., Niu, M., Reimer, R.W., Richards, D.A., Scott, E.M., Southon, J.R., Staff, R.A., Turney, C.S.M., van der Plicht, J., 2013. IntCal13 and Marine13 radiocarbon age calibration curves 0–50,000 years cal BP. Radiocarbon 55, 1869–1887.
Rodgers, K.B., Aumont, O., Madec, G., Menkes, C., Blanke, B., Monfray, P., Orr, J.C., Schrag, D.P., 2004. Radiocarbon as a thermocline proxy for the eastern equatorial Pacific. Geophysical Research Letters 31, L14314.
Russell, N., Cook, G.T., Ascough, P.L., Scott, E.M., Dugmore, A.J., 2011. Examining the inherent variability in ΔR: new methods of presenting ΔR values and implications for MRE studies. Radiocarbon 53.
Sadler, J., Carré, M., Azzoug, M., Schauer, A.J., Ledesma, J., Cardenas, F., Chase, B.M., Bentaleb, I., Muller, S.D., Mandeng, M., Rohling, E.J., Sachs, J.P., 2012. Reconstructing past upwelling intensity and the seasonal dynamics of primary productivity along the Peruvian coastline from mollusk shell stable isotopes. Geochemistry, Geophysics, Geosystems 13, Q01015.
Siani, G., Michel, E., De Pol-Holz, R., DeVries, T., Lamy, F., Carel, M., Isguder, G., Dewilde, F., Lourantou, A., 2013. Carbon isotope records reveal precise timing of enhanced Southern Ocean upwelling during the last deglaciation. Nature Communications 4.
Silva, N., Rojas, N., Fedele, A., 2009. Water masses in the Humboldt Current System: properties, distribution, and the nitrate deficit as a chemical water mass tracer for equatorial subsurface water off Chile. Deep Sea Research Part II: Topical Studies in Oceanography 56, 1004–1020.
Southon, J.R., Oakland Rodman, A., True, D., 1995. A comparison of marine and terrestrial radiocarbon ages from northern Chile. Radiocarbon 37, 389–393.
Strub, P.T., Mesias, J.M., Montecino, V., Rutllant, J., Salinas, S., 1998. Coastal ocean circulation off western South America. In: Robinson, A.R., Brink, K.H. (Eds.), The Global Coastal Ocean. Regional Studies and Syntheses. Wiley, New York, pp. 273–315.

Stuiver, M., Polach, H.A., 1977. Discussion; reporting of C-14 data. Radiocarbon 19, 355–363.
Tarifeño, E. (1980). "Studies on the Blology of Surf Clam *Mesodesma donacium* (Lamarck, 1818) (Bivalvia: Mesodesmatidae) from Chilean Sandy Beaches." Unpublished PhD thesis, University of California.
Taylor, R.E., Berger, R., 1967. Radiocarbon content of marine shells from the Pacific coasts of Central and South America. Science 158, 1180–1182.
Toggweiler, J.R., Dixon, K., Broecker, W.S., 1991. The Peru upwelling and the ventilation of the South Pacific thermocline. Journal of Geophysical Research 96, 20,467–20,497.
Torres, R., Pantoja, S., Harada, N., González, H.E., Daneri, G., Frangopulos, M., Rutllant, J.A., Duarte, C.M., Rúiz-Halpern, S., Mayol, E., Fukasawa, M., 2011. Air–sea CO2 fluxes along the coast of Chile: from CO2 outgassing in central northern upwelling waters to CO2 uptake in southern Patagonian fjords. Journal of Geophysical Research, Oceans 116, C09006.
van Beek, P., Reyss, J.-L., Paterne, M., Gersonde, R., van der Loeff, M.R., Kuhn, G., 2002. 226Ra in barite: absolute dating of Holocene Southern Ocean sediments and reconstruction of sea–surface reservoir ages. Geology 30, 731–734.
Wang, D., Gouhier, T.C., Menge, B.A., Ganguly, A.R., 2015. Intensification and spatial homogenization of coastal upwelling under climate change. Nature 518, 390–394.
Ward, G.K., Wilson, S.R., 1978. Procedures for comparing and combining radiocarbon age determinations: a critique. Archaeometry 20, 19–31.
Weiss, R.F., 1974. Carbon dioxide in water and seawater: the solubility of a non-ideal gas. Marine Chemistry 2, 203–215.

https://doi.org/10.1016/j.yqres.2015.12.002 Published online by Cambridge University Press